TASK QUARTERLY 3 No 3 (1999), 343–360

APPLICATION OF THE VORTEX–IN–CELL METHOD FOR THE SIMULATION OF TWO–DIMENSIONAL VISCOUS FLOW

HENRYK KUDELA

Wroclaw University of Technology,
Wybrzeze Wyspianskiego 27,
50–370 Wroclaw, Poland

Abstract: In the paper the vortex in cell method for the simulation of the viscous flow in a complex geometry was described. Vorticity field is approximated by the collection of the particles that carries the circulation. The local velocity of a particle was obtained by the solution of the Poisson equation for the stream function by the grid method and then interpolation of velocity from the grid nodes to the vortex particle position. The Poisson equation for the stream function was solved by fast elliptic solvers. To be able to solve the Poisson equation in a region with a complex geometry, the capacitance matrix technique was used. The viscosity of the fluid was taken in a stochastic manner. A suitable stochastic differential equation was solved by the Huen method. The non–slip condition on the wall was realized by generation of vorticity. The program was tested by solving several flows in channels of different geometry and at a different Reynolds number. Here we present the testing results concerning the flow in a channel with sudden symmetric expansion, for the flow in channel with backward step, and the flow over building systems.

Keywords: vortex–in–cell, viscous flow, generation of vorticity, stochastic differential equations

1. Introduction

The vortex method belongs among the particle methods. It means that for the solution of the equation of motion we utilized the "particles" that are called vortex, which serve as a carrier of circulation [5, 6, 9, 15, 19, 25]. The calculations were carried out in lagrangian coordinates. Generally the vortex methods are divided into the direct method, in which the velocity of the vortex particle is calculated by the summation of the contribution from all particles that exist at the flow by virtue of the Biot–Savart law [7], and the method called vortex–in–cell method [9]. Due to the fact that the number of operations in the direct vortex method is in each time step proportional to the square of the number of particles that are in the flow $\sim O(N^2)$, computational time for solutions of the specific problems is very large. On

the other hand, in the vortex in cell method [9], the velocity is calculated through differentiation of the stream function, which is obtained by the solution of the Poisson equation on the numerical grid. The number of operations per one time step is proportional to $O(N+M\log M)$, where M is the number of points on the mesh, and that results in essentially reducing the computational time. Here we described the vortex–in–cell method. We wrote the general proposed program on the basis of the vortex in cell method and tested it solving several problems, and then compared the results with experimental data or with numerical results obtained by a different method.

2. Description of the Vortex–in–Cell Method

The non–dimensional equations of incompressible fluid motion in two–dimensional space transformed to the vorticity transport equations [7] take the form:

$$\frac{\partial \omega}{\partial t} + (\mathrm{u} \cdot \nabla)\omega = \frac{1}{Re}\Delta\omega, \tag{1}$$

$$\Delta\psi = -\omega, \qquad u = \frac{\partial \psi}{\partial y}, \qquad v = -\frac{\partial \psi}{\partial x}, \tag{2}$$

where ω is the non–zero component of the vorticity vector, $\mathbf{u} = (u,v)$ is the velocity divided by the uniform inlet velocity U, ψ is the stream function, t — is the time, and Re is the Reynolds number defined as $Re = Uh/v$, where v is the coefficient of kinematic viscosity.

The vortex method is based on the so–called viscous splitting algorithm. First, the Euler equation ($v = 0$) is solved; then the diffusion equation is solved. Due to the fact that the diffusion is taken into account in the stochastic manner, we can interpret the equation of fluid motion in terms of the stochastic processes. One can note that due to the incompressibility of the fluid, $\nabla \cdot \mathbf{u} = 0$, the equation (1) can be rewritten as:

$$\frac{\partial \omega}{\partial t} + \nabla \cdot (\mathbf{u}\omega) = \frac{1}{Re}\Delta\omega. \tag{3}$$

Equation (3) is identical, with respect to form, to the forward Kolmogorow–Fokker–Planck equation that describes the probability density called transition density for the stochastic (Markov) process [17]:

$$P(X(t) \in A, t) = \int_A G(x, t; \alpha, 0)\, dx, \tag{4}$$

where P is probability, $G(x,t;\alpha,0)$ is a solution of equation (3). In the theory of the stochastic differential equation, it is shown that the stochastic process that is described by a stochastic differential equation (in the Ito sense) [17]:

$$dX(t) = \mathrm{u}(x,t)\,dt + \sqrt{\frac{2}{Re}}\,dW, \tag{5}$$

has the transition density function that satisfies equation (3), where W means the Wiener process. So equation (5) described the convection and diffusion process and can be regarded as the fluid motion equation.

For the solution (5) we used a viscous splitting algorithm [6, 19]: velocity (drift) is calculated for inviscid flow and the last term is added in order to take into account the diffusive property of the viscosity of the fluid. In the present work instead of the commonly used Euler scheme that has the order of convergence of only 0.5, for the solution of equation (5) we use the generalized Huen scheme that has the order one [17]:

$$x_p^{n+1} = x_p^n + \frac{1}{2}\left(u^n(x_p^*) + u^n(x_p)\right)\Delta t + \sqrt{\frac{2}{Re}\,\Delta t}\,\Delta W_n, \tag{6}$$

where $x_p^* = x_p + u^n(x_p)\,\Delta t + \sqrt{\frac{2}{Re}\,\Delta t}\,\Delta W_n$, ΔW_n is an increment of the Wiener process, and Δt is a time step. It is well known that the increments of the Wiener process are the independent Gaussian random variables with mean $E(\Delta W_n) = 0$ and variance $E((\Delta W_n)^2) = \Delta t$; so it is relatively easy to generate it by pseudo–random generator of numbers with uniform distribution and using the Box–Muller transformation [17].

Now we describe the vortex–in–cell (VIC) algorithm for obtaining the inviscid velocity field $\mathbf{u}(u,v)$. Vorticity $\omega(x,y)$ is approximated by the linear combination of the Dirac measures:

$$\omega^n(x) = \sum_p \Gamma_p \delta(x - x_p^n), \qquad \Gamma_p = h^2 \omega^n(x_p), \tag{7}$$

where p is the number of the vortex particle. Approximation (7) is understood in the sense of measure on R^2 [25]:

$$\int \omega(x)dx \approx \sum_p \omega(x_p)\,h^2. \tag{8}$$

We assumed that we were able to solve the Poisson equation for the stream function (2) by the finite difference method. The computation goes as follows:

1. At first the redistribution of the mass of vortex particles on the grid nodes is done:

$$\Gamma_j^n = \sum_p \Gamma_p \varphi_j(x_p^n), \tag{9}$$

where $\varphi_j(x) = \varphi((x - x_j)/h)$, is a B–spline of order m [26, 18]. For $m = 1$ the B–spline has the form:

$$\varphi(x)=\begin{cases} 1-|x| & for\ \ |x|\le 1 \\ 0 & for\ \ |x|>1, \end{cases} \tag{10}$$

and the redistribution process (9) corresponds to a well known area–weighted interpolation scheme [8]. In the present work we use the B–spline of the first order in the cells that adjoin the boundary of the domain flow and outside these cells we used the B–spline of the 3rd order that takes the form [18, 26]:

$$\varphi(x)=\begin{cases} \frac{1}{2}|x|^3-x^2+\frac{2}{3}, & |x|\le 1 \\ -\frac{1}{6}|x|^3+x^2-2|x|+\frac{4}{3} & 1<|x|<2 \\ 0 & |x|\ge 2. \end{cases} \tag{11}$$

The B–splines satisfy: $\varphi(x) = \varphi(-x)$ and $\int\varphi(x)dx=1$. To obtain the vorticity in the grid node, we should divide the circulation of the node obtained from (9) by the volume of the cell h^2. Instead of this, in order to overcome some difficulties related to the accumulation of the particles, Cottet [10] proposed the calculation of the volume of the node through position of the particles around the node:

$$J_j=\sum_p h^2\varphi_j(x_p)=\sum_p h^2\ \varphi\left(\frac{x_j-x_p}{h}\right). \tag{12}$$

Then the vorticity in j node is calculated as:

$$\omega_j=\frac{\Gamma_j}{J_j}=\frac{\sum_p \Gamma_p\ \varphi_j(x_p)}{\sum_p h^2\varphi_j(x_p)} \tag{13}$$

2. We solved the Poisson equation for the stream function with a boundary condition that assured cancellation of the normal component of the velocity field on the wall (ψ = const, e.g $\psi = 0$ and $\psi = Q$, where Q is a flow rate)

$$\Delta\psi=-\omega. \tag{14}$$

The velocity at the grid nodes is calculated by central difference:

$$\begin{aligned} u_j&=-\frac{\psi(x_{j_1},y_{j_2}+h)-\psi(x_{j_1},y_{j_2}-h)}{2h}, \\ v_j&=\frac{\psi(x_{j_1}+h,y_{j_2})-\psi(x_{j_1}-h,y_{j_2})}{2h}. \end{aligned} \tag{15}$$

3. The value of the velocity from the grid nodes is interpolated to the position of the particles:

$$u^n(x_p) = \sum_{j \in J^2} u_j^n l_h(x_p - x_j), \tag{16}$$

where l_h is the base function of the lagrangian interpolation. In the present work we took as $l_h(x)$ the B–spline $\varphi(x)$ of order one. This ends the computation process for the VIC algorithm.

To satisfy the non–slip condition on the wall ($\partial\psi/\partial n = 0$) we utilised the vorticity generation process. In numerical practice when fluid equations are formulated in $\psi - \omega$ terms, one comes across the problem of the determination of the vorticity value on the wall. In literature we can find a whole family of different approximate formulas allowing one to make this [13, 23]. One of the oldest and simplest is the Thom's formula [23]:

$$\omega_B = -\frac{2}{\Delta y^2}\psi_{i,1}. \tag{17}$$

Formula (17) may be obtained from equation (14) when one writes it on the wall and takes into account the fact that $(\psi_{i,1} - \psi_{i,-1})/(2\Delta y^2) = 0$ (index -1 is related to the "ghost" point outside the computational domain). At each time step it is assumed that the formula designates the proper amount of vorticity on the wall. If old vortex particles that already exist in the flow give to the boundary point (by redistribution) the vorticity ω_{old} then to the nodes point on the boundary the new portion of vorticity is added:

$$\omega_B = \omega_{new} + \omega_{old}. \tag{18}$$

The new portion of vorticity ω_{new} is redistributed among the n_v vortex particles giving them the circulation $\Gamma = (\omega_{new} h^2)/n_v$ where n_v was chosen in such a way that $|\Gamma| < 0.05$, ($n_v = 2 \div 11$). A similar process generation of vorticity was successfully applied in papers [5, 28].

Instead of formula (17) the Woods formula was also tested: $\omega_B = -3\psi_1/\Delta y^2 - (1/2)\omega_1$ [13, 23], where ψ_1, ω_1 correspond to the stream function and vorticity values at distance Δy from the wall. Woods formula has the same order of accuracy and gave results similar to the Thom's formula (17).

The final step in obtaining the solutions is the displacement of the vortex particles in accordance with formula (6), and the whole process begins again from step 1.

For the solution of the Poisson equation fast elliptic solver was used. To be able to solve the Poisson equation in irregular region capacitance matrix technique was used. The capacitance matrix technique is well described in many places in literature [3, 24, 27].

3. Exemplary Numerical Results

3.1 Flow in channel with sudden expansion

At first we will present the results related to flow over the plane symmetric expansion (Figure 1).

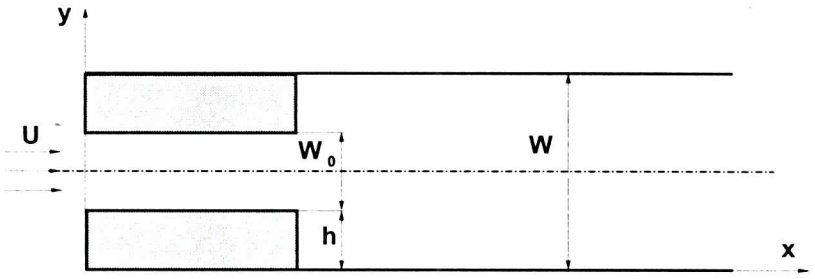

Figure 1. *Skech of the geometry for the flow over a plane symmetric sudden expansion*

The length of computational domain was taken as $32h$, where $h = 1$ is the height of the step. The expansion ratio was W_0/W=1/3 or 1/2.

From the literature it is known that as the Reynolds number is increased the flow undergoes several changes [4, 12, 14]. For a small Reynolds number, ($Re \approx 56$) the lengths of separation regions behind each step are equal and velocity profiles are symmetrical. The growth of the Reynolds number ($Re \approx 125$) causes the loss of symmetry. One of the recalculation zones becomes larger. Further growth of the Reynolds number ($Re \approx 252$) causes changes in the picture of the flow that are explained in the term of a bifurcation theory [14], Figure 2.

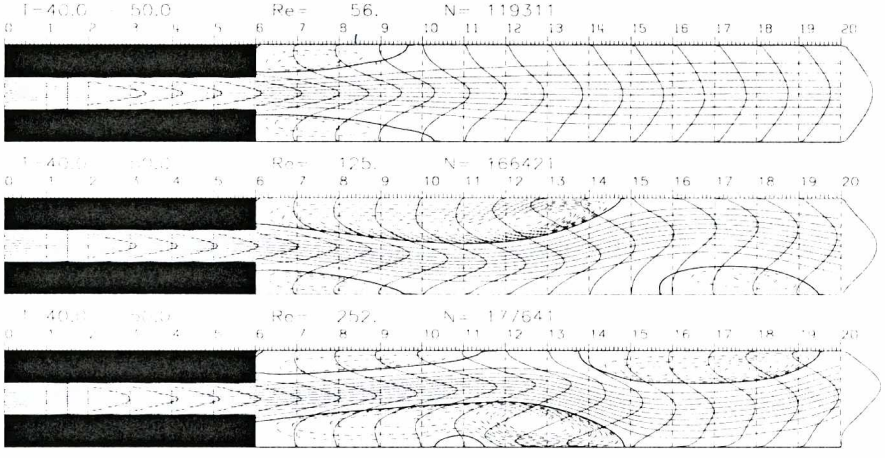

Figure 2. *Averaged streamlines with velocity profiles at Re=56, Re=125 and Re=252, W=3h, W_0=h. Dashed lines mean the streamlines have values less than zero or greater than 1*

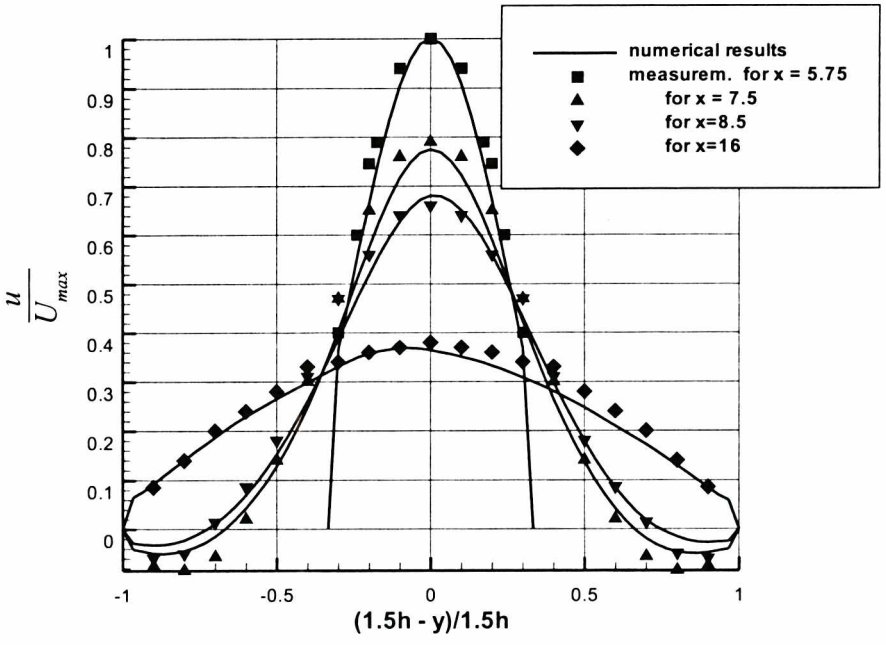

Figure 3. *Comparison of the numerical results of velocity distribution across the vertical section with measurements taken from [12], Re=56, $W_0/W=1/3$*

Calculated velocity distributions across a vertical cross section of the channel for different values of x for $Re = 56$ were compared with experimental measurements published in paper [12] and it is presented in Figure 3. The agreement is good but one may notice that the distribution of the velocity near the wall is not as smooth as we had expected it to be.

The vortex method provides a natural possibility for visualization of the flow and its analysis in terms of vorticity distribution by tracing the position of the vortex particles. Figure 4 presents the sequence of the vortex particle positions at $Re = 1000$, $W_0/W = 1/2$. For T = 40 we can see very clearly the vortex structures that are in good qualitative agreement with the results presented in work [4] (see Figure 5). We used the red color (dark and light) for marking the vortex particles of the negative sign, and the blue color (dark and light) for the positive sign of vortex particles. The darker points correspond to the value of circulation that is greater than the mean value, calculated separately for positive and negative vortex particles.

We also carried out the calculation for flow at a very high Reynolds number ($Re = 10^5$). We must say that we are conscious of the objections, which correspond to the problem of numerical diffusion, the resolution and so on. The aim of these numerical experiments was just to check the possibility of the VIC method for modeling of such a flow. As it was pointed out by Chorin [8], one should keep in mind the difference between modelling with vortices and numerical approximations of solution of a fluid motion equation by the vortex method. It seems that the last

experiment belongs to the "modelling". This means we tried with the help of a moderate number of vortices to get qualitative understanding of the vorticity field dynamic at a very high Reynolds number. The sequence of the vortex particles for the flow at $Re = 10^5$ is presented in Figure 6. It is easy to notice the presence of vorticity filaments — thread–like structures that are regarded as typical structures of two–dimensional turbulence [2, 16, 20, 22]. One can observe that filaments are accompanied by a large coherent vortex structure that stabilises them, [16, 20, 22]. These large vortex structures are build with both sings of vortex particles. Vortices of the same sign may undergo merging and vortices of opposite sign may form dipoles [20, 22].

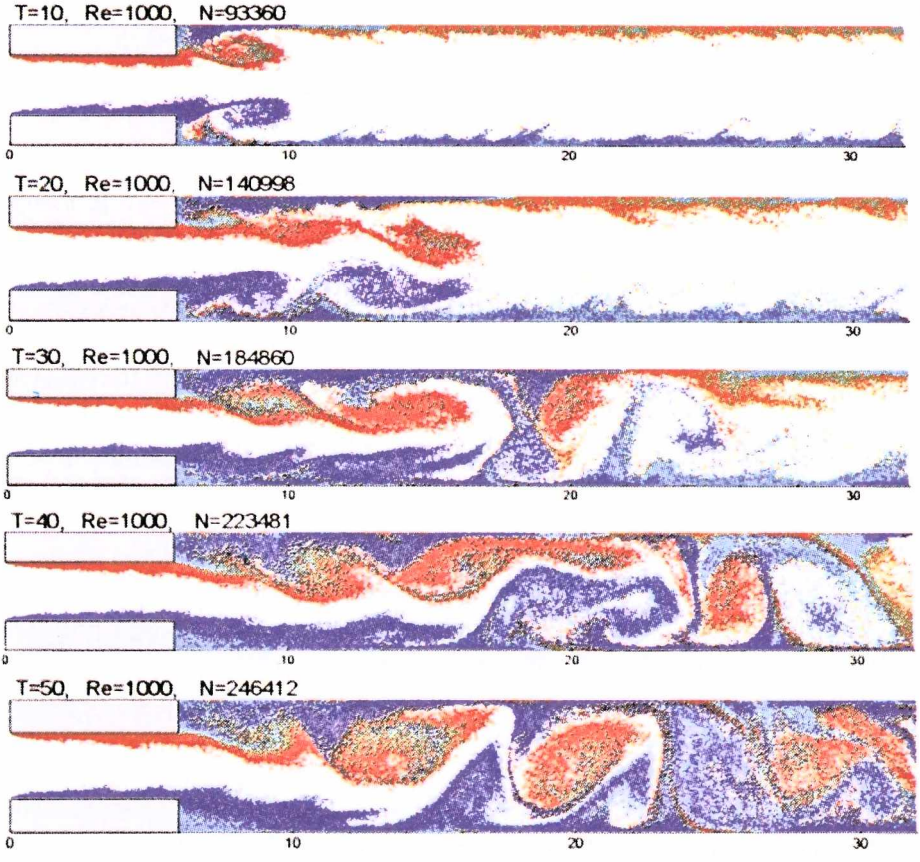

Figure 4. *Evolution of the vorticity in channel with sudden symmetric expansion, Re=1000, $W_0/W=1/2$. N means the number of particles*

Figure 5. *Scanned picture of the experimental visualization from the Cherdron, Drust, and Withelow paper [4](Figure 9d)*

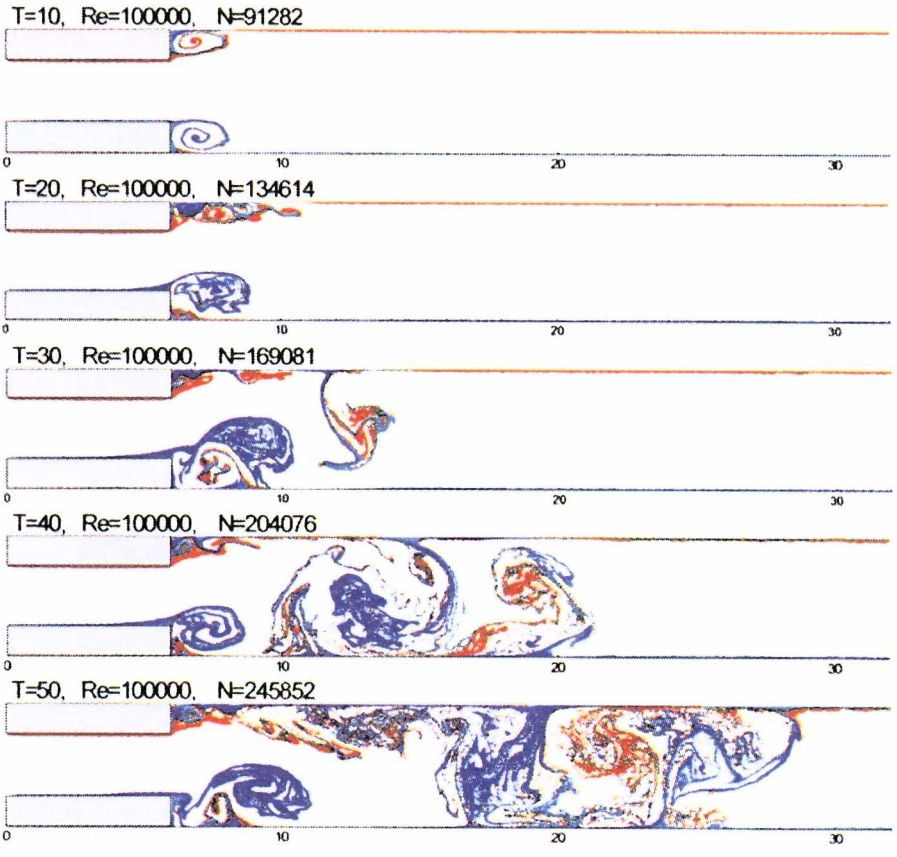

Figure 6. *The sequence of the vortex particle position at Re=100000, W_0 / W=0.5*

3.2 Flow over the backward–facing step

For the flow over the backward–facing step there are well–documented experimental [1, 11] and numerical data [15, 21] available from literature. So this flow is a good example for testing the program. At first we checked the lengths of the recirculation zone behind the step at different Reynolds number. It is known that the reattachment length $x_r = x_1/H_s$ (see Figure 7) increases approximatly linearly as the Reynolds number increases.

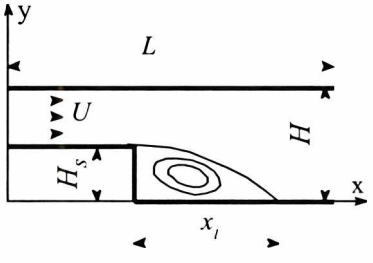

Figure 7. *Sketch of the geometry for the flow over backward–facing step*

In Figure 8 we showed the averaged streamlines for different Reynolds numbers (Re = 100, 200, 300, 400, 500, 600). For calculation purposes we took Δt = 0.01, $\Delta x = \Delta y = 0.05$, $L = 12H$, $H = 1$, $U = 1$. To reduce the statistical perturbations due to stochastic manner of solution of the diffusion equation we carried out an averaging process. The averaging was done for 200 time steps form T=38÷40. The linear growth of the recirculation zone is visible. For Reynolds number $Re < 300$ the agreement with the experiments are very good [1, 11] but for $Re > 300$ the length of the recirculation zone is underestimated.

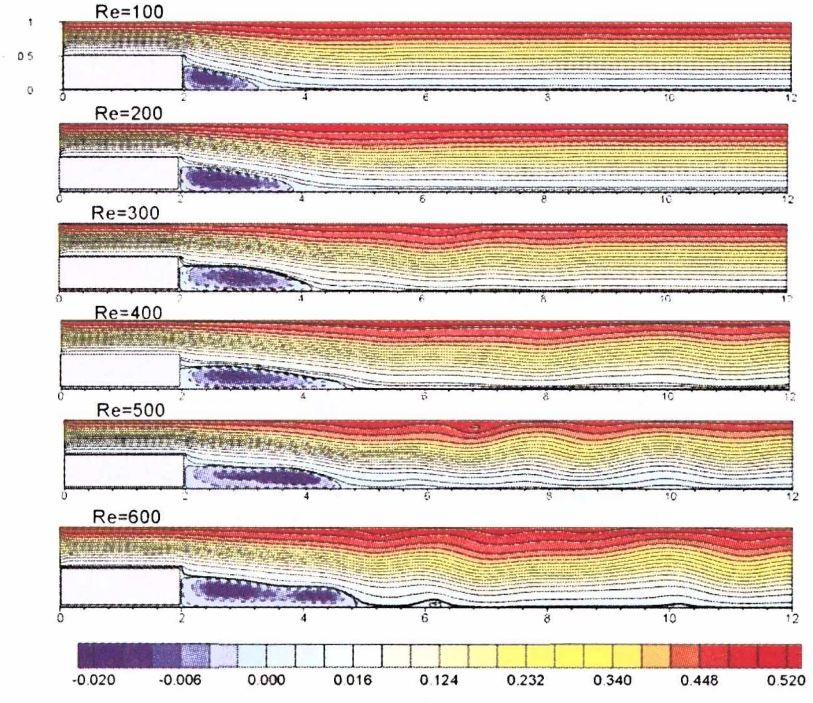

Figure 8. *Averaged streamlines at Re = 100, 200, 300, 400, 500, 600, t ∈ [38,40], Δ t=0.01*

It is difficult to indicate one special reason for that. It is known that for Reynolds number $Re \propto 229$ [11] the velocity starts to oscillate near the re–attachment point. Due to vorticity generation on the wall and the stochastic manner of simulation of viscosity of the fluid, the flow is permanently perturbed and it is difficult to determine precisely the position of the re–attachment point. The same effect was observed, in the direct vortex method used for the simulation of this flow [19].

In order to see the qualitative changes that the vorticity field undergoes when the Reynolds number increased we present in Figure 9 the vorticity field created by the vortex particle position at different Reynolds numbers in the same time T = 40. In the first frame (Re = 100), the vortex particles are uniformly spread throughout the channel. When the Reynolds number increases, we see that a potential core (the space without any vortex particles) appears. This potential core grows when the

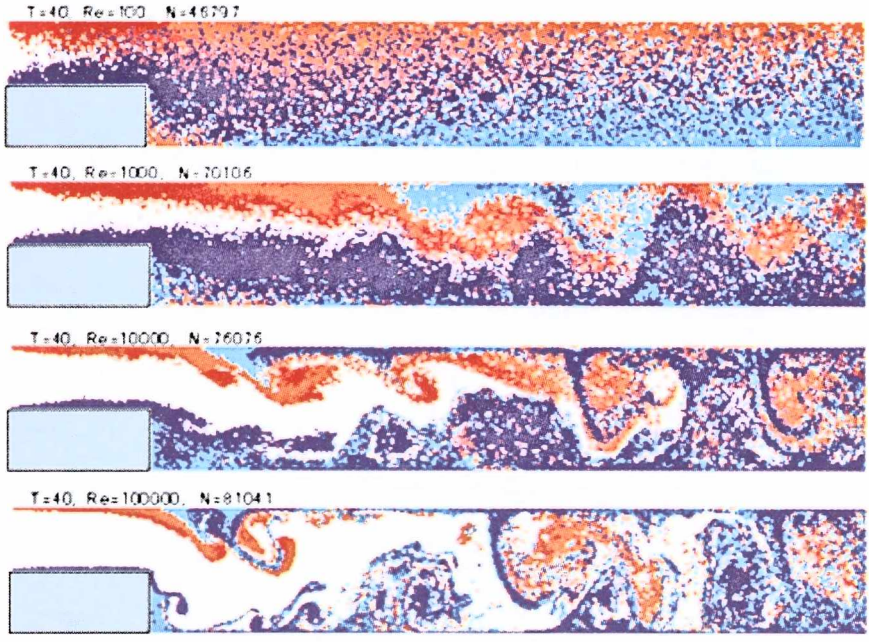

Figure 9. *The vorticity field created by vortex particle positions at different Reynolds number and in the same dimensionless time T=40*

Reynolds number is increased. It is easy to notice the filaments of vorticity and the large vortex structure at high Reynolds numbers.

In Figure10 the sequence of the instantaneous vortex particle position was shown at Reynolds number $Re = 10^5$. It is interesting to notice the vorticity shedding phenomena from the point on the upper wall (opposite to the corner of the step). The remarks that were made at the end of section 3.1 about the behaviour of the vorticity at large Reynolds numbers is also true in this case. The vorticity has a tendency to create filaments. We see that filaments are accompanied by large coherent vortex structures that stabilize them, and vortices of the opposite sign form a dipole structure [20, 22, 16]. These large vortex structures are built with both positive and negative signs of vortex particles.

3.3 Flow over a system of buildings

In paper [29] interesting pictures of the flow over the system of buildings were published. The flow was visualized using smoke (see Figure 11 for scanned pictures from that paper). The pictures illustrate how minor design modifications can make a large difference in wind velocity at the pedestrian level (between the building). In the paper [29] there was a notice that "the high buildings cause the high velocities by deflecting the upper and faster atmospheric layers down to the ground; where they impinge on the ground, the velocities may be double the value they would be in the absence of the building".

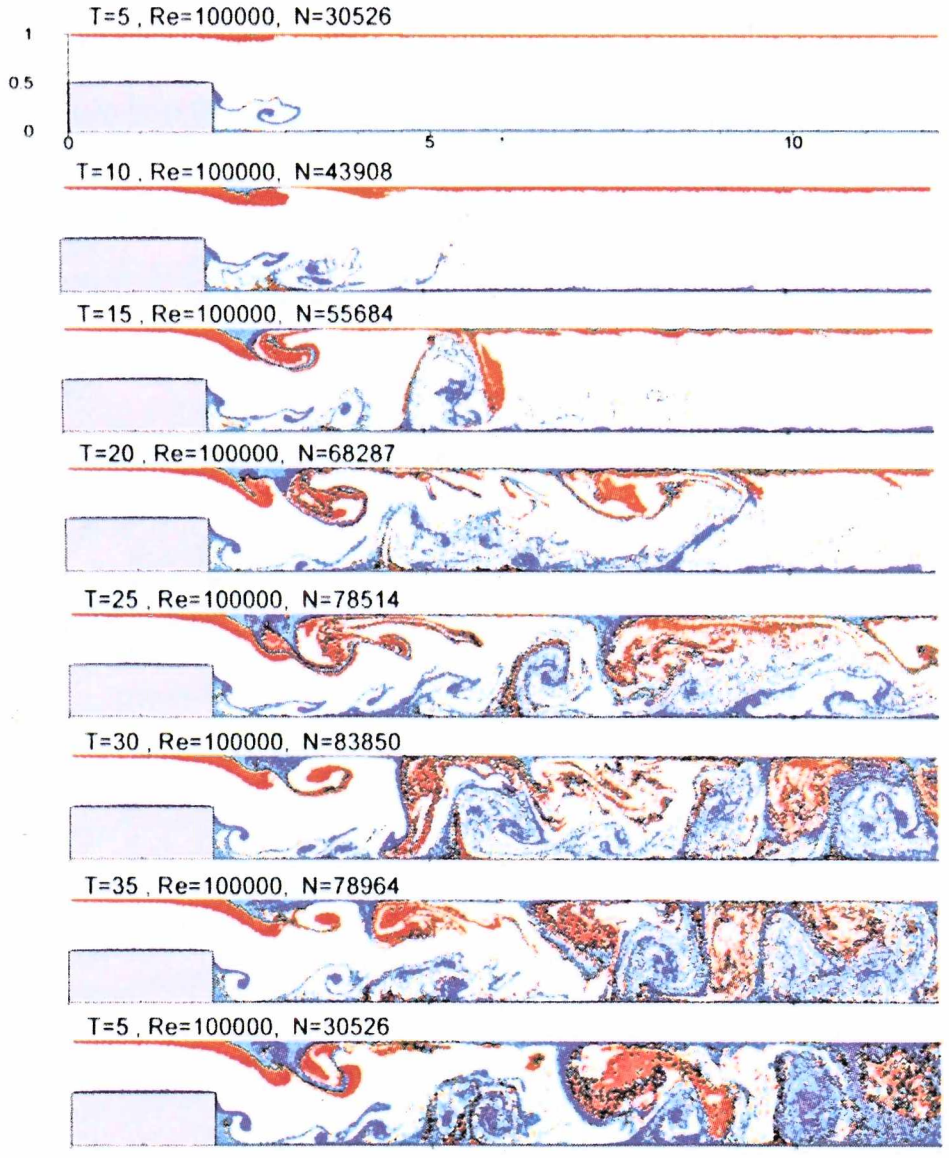

Figure10. *The sequence of the vortex particle positions in channel over backward–facing step, $Re=10^5$*

Figure 12 shows the scheme of the configuration of the buildings that was taken to the calculation. As a unit length the height h of the smaller building was taken, $h = 1$. The height of the higher building was $3h$. At the inlet the velocity $U = 1$, $Re = Uh/v$ was taken. The dimension of the computational domain was taken $15h \times 6h$. On the upper boundary it was presumed that the normal velocity is zero. So the generation of the vorticity took place only at the rigid boundary at the bottom and on the surface of the building. Gird steps was taken as $\Delta x = \Delta y = 0.1$, $\Delta t = 0.01$.

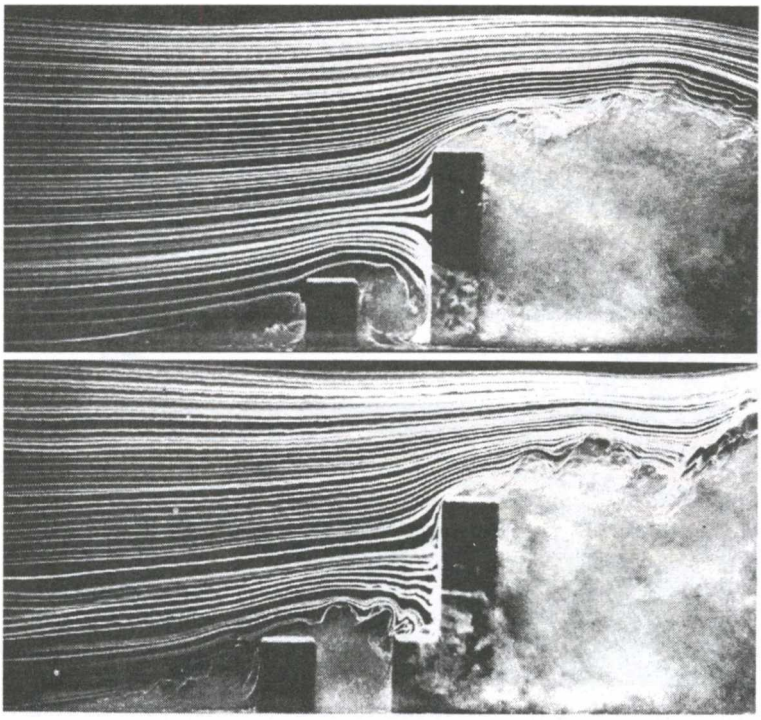

Figure 11. *Scanned pictures of the flow visualization around two models of tall buildings taken from the paper by H.Thomann [29]*

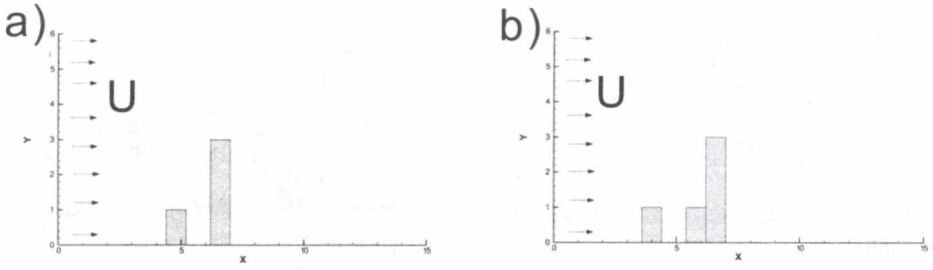

Figure 12. *The scheme of the computational domain for the flow over the system of buildings: a) the plain system of buildings b) modified system of buildings*

Figure 13 shows the streamlines that were obtained by vortex method. The shapes of the streamlines and generated structures are in good qualitative agreement with the experimental pictures presented in Figure 11. For numerical calculation we choose $Re = 2000$, $Re = Uh/v$.

The vortex method has the natural possibility of analyzing the flow features in term of vorticity through vortex particle positions. In Figures 14 and 15 the sequence of the vortex particle positions for the plain (unmodified) and modified system of building was presented. We started the calculation from the potential flow. For $t > 0$ the viscosity of the fluid started to play a role. One can see the development of the Kelvin–Helmholtz type vortex structure. This vortex structure

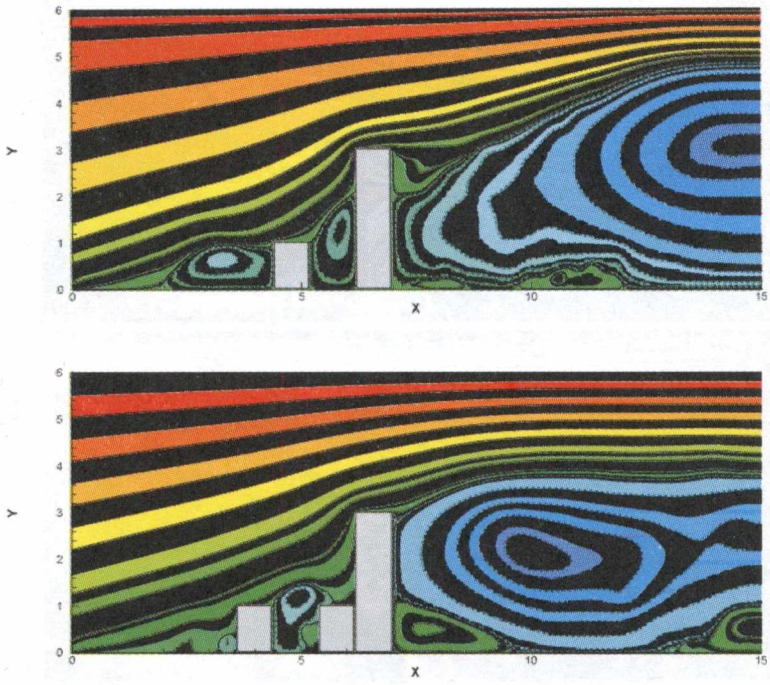

Figure13. *Streamlines of the flow over the buildings obtained from the calculation. To visualize the structures of streamlines better, the zebra technique of drawing was used*

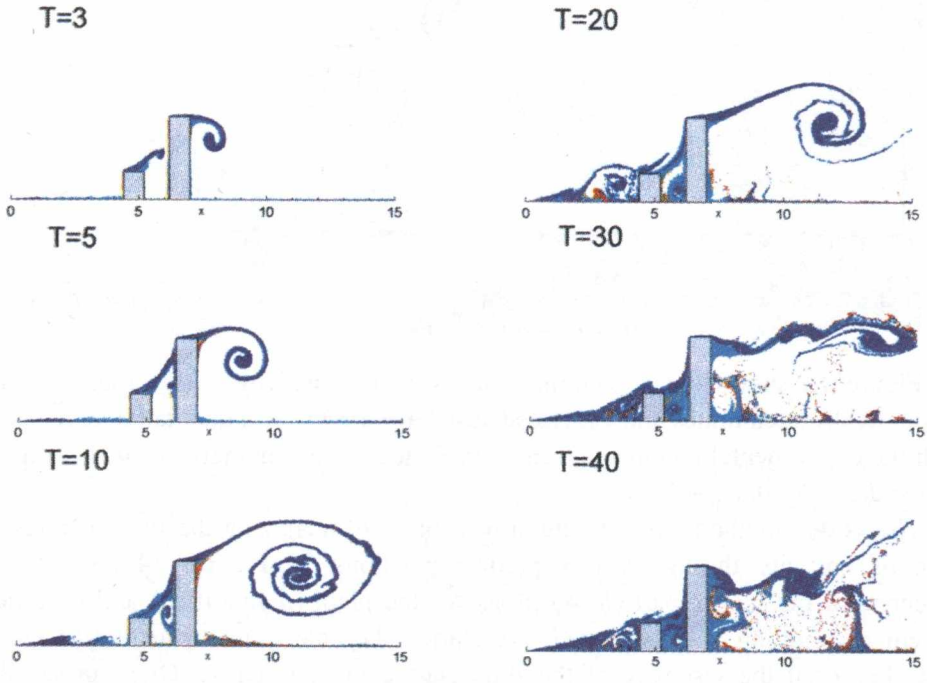

Figure 14. *The sequence of the instantaneous positions of the vortex particles, Re=10000*

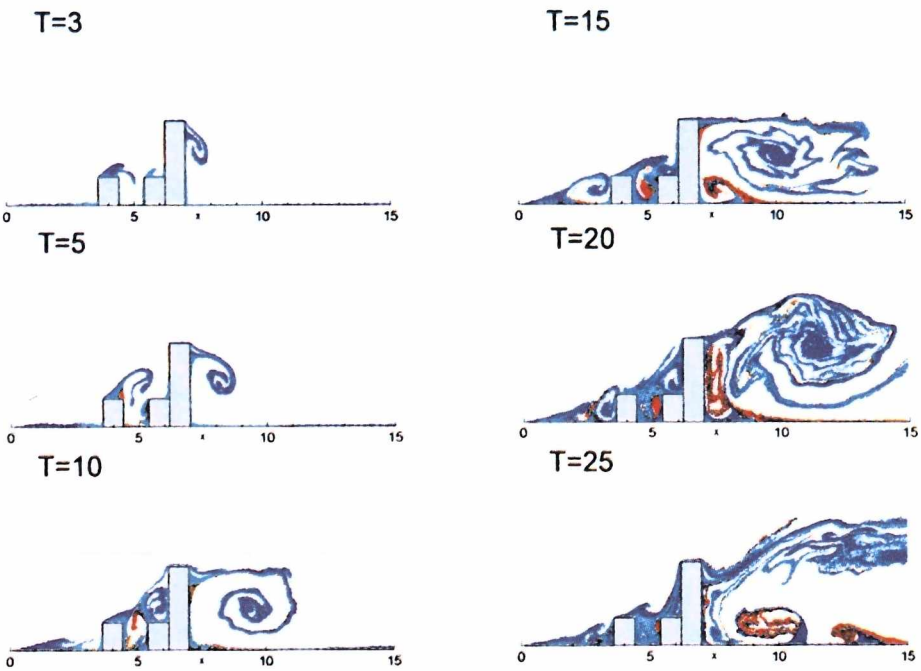

Figure 15. *The sequence of the instantaneous positions of the vortex particles for modified structure of buildings, Re=10000*

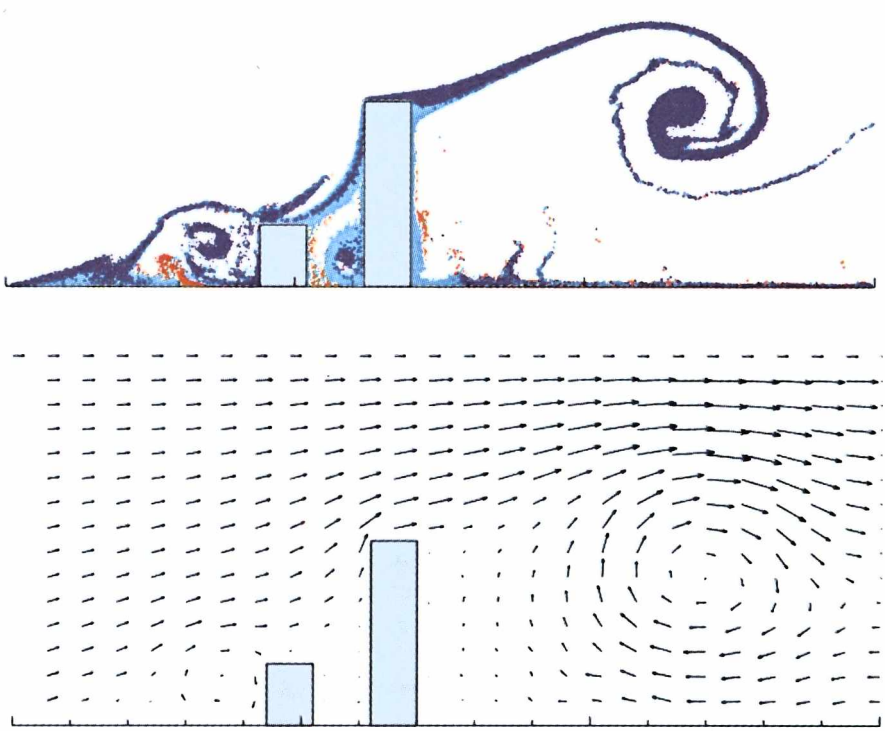

Figuire16. *Instantaneous vorticity field that was created by the vortex particle positions and related to its velocity field*

induced an air velocity greater than the velocity of the air coming toward the fronts of the buildings. This is clearly visible in Figure 16, where the close-up of the frame for T = 20, together with the velocity field, was presented.

A small element in front of the tall building was added to lower the velocity on the pedestrian level between the buildings. That velocity was reduced several times. It is interesting to notice the influence of that small construction on the vorticity distribution behind the tall building (compare the relevant frames in Figures 14 and 15). We notice that the added construction destabilized the vortex Kelvin–Helmholtz structure, and the distribution of the vorticity behind the tall building is more chaotic.

4. Concluding Remarks

It seems that now it is not far from the creation of a general flow simulation package based on the vortex method into which the user needs only enter minimal data concerning boundaries in order to be able to perform the numerical investigations. The present paper is a move in that direction. Vortex methods provide natural, useful tools for analysing flow in terms of vorticity dynamics, and the visualisation of the flow by vortex particles. The study of the evolution of the vorticity field helps one to understand the features of flow in a complicated geometry. It is one of the few methods which give reasonable results at large interval of Reynolds numbers trying to solve the Navier–Stokes directly. Further study on the VIC method should clarify the problem of numerical diffusion that may be introduced by a numerical grid. It is believed that the introduction of the deterministic method of the diffusion simulation instead of stochastic one should improve the numerical results.

References

[1] Armaly B.F., Durst f., Pererira J.C., Schönung B., *Experimental and Theoretical Investigations of Backward–Facing Step Flow*, J. Fluid Mech., vol. 127, pp.473–496, (1983)

[2] Brachet M.E., Meneguzzi M., Politano H., Sulem P..L., *The dynamics of freely decaying two–dimensional turbulence*, vol. 194, pp. 333–349, (1988)

[3] Buzbee B. L., Dorr F.W., George J. A., Golub G. H., *The solution of the discrete Poisson equation on irregular regions*, SIAM, J. Num. Anal., vol. 8, pp. 722–736, (1971)

[4] Cherdron W., Durst F., Whitelaw J.H., *Asymmetric flows and instabilities in symmetric ducts with sudden expansions*, J.Fluid Mech., vol. 84, pp. 13–31, (1978)

[5] Chang C. C., Chern R.–L., *A numerical study of flow around an impulsively started circular cylinder by a deterministic vortex method*, J. Fluid Mech., vol. 233, pp. 243–263, (1994)

[6] Chorin A. J., *Numerical Study of Slightly Viscous Flow*, J. Fluid Mech. Vol. 57, pp. 785–796, (1973)

[7] Chorin A.J., Marsden J.E., *A Mathematical Introduction to Fluid Mechanics*, Springer (1979)

[8] Chorin A. J., *Microstructure, renormalization, and more efficient vortex methods*, ESAIM, Proceedings, Vortex Flows and Related Numerical Methods II, 96, Vol. 1, pp. 1–14, (1996), http, // www.emath.fr/proc/ Vol.1/contents.htm

[9] Christiansen J.P., *Numerical simulation of Hydrodynamics by the Method of Point Vortices*, J.1 Comp. Phys., vol. 13, pp. 363–379, (1973)

[10] Cottet G-H. A., *A particle–grid superposition method for the Navier–Stokes equations*, J. Comp. Phys., vol. 89, pp. 301–318, (1980)

[11] Denham H.K., Patrick M.A., *Laminar flow over a downstream–facing step in a Two–dimensional Flow Channel*, Trans. Instn Chem. Engrs., vol.52, pp. 361–367, (1974)

[12] Durst F., Melling A., Whitelaw J.H., *Low Reynolds number flow over a plane symmetric sudden expansion*, J. Fluid Mech., vol. 64, pp. 111–128, (1974)

[13] E Weinan, Liu Jian–Guo, *Vorticity boundary condition and related issues for finite difference schemes*, J. Comput. Phys., vol 124, pp. 368–382, (1996)

[14] Faren R.M., Mullin T., Cliffe K.A., *Nonlinear flow phenomena in a symmetric sudden expansion*, J.Fluid Mech., vol. 124, pp. 368–382, (1990)

[15] Ghoniem A.F., Cagnon V., *Vortex Simulations of Laminar Recirculating Flow*, J. Comp. Phys., vol.68, pp. 348–377, (1987)

[16] Kevlahan N. K.–R. Farge M., *Vorticity filaments in two–dimensional turbulence, creation, stability and effect*, J. Fluid Mech., vol. 346, pp. 49–76, (1997)

[17] Kloeden P., Platen E., *Numerical Solution of Stochastic Differential Equations*, Springer, 1982

[18] Kong J. X., *Contribution a l'analyse numericque des methodes de couplage particules–grille en mecanique des fluides*, Phd. dissert., Universite J. Fourier Grenoble, LMC–IMAG (1993)

[19] Kudela H., *Numerical modelling of the hydrodynamic phenomena by vortex methods*, Monographs 25 (1995), Oficyna Wydawnicza Politechniki Wroclawskiej, Wroclaw 1995

[20] Lesieur M., *Turbulence in Fluids*, Third edition, Kluwer Academic Publishers, (1997)

[21] Kaiktsis L., Karniadakis G.E., Orszag S. A., *Onset of three–dimensionality, equilibria, and early transition in flow over a backward–facing step*, J. Fluid Mech. Vol. 231, pp. 501–528, (1991)

[22] McWilliams J.C., *The emergence of isolated coherent vortices in turbulent flow*, J. Fluid Mech., vol. 146, pp. 21–46, (1984)

[23] Peyret R., Taylor T. D., *Computational methods for fluid flow*, Springer–Verlag (1983)

[24] Proskurowski W., Widlund O., *On the numerical solution of Helmholtz's equation by the capacitance matrix method*, Math. Comput., vol.30, pp.433–468, (1976)

[25] Raviart P.A., *An analysis of particle methods, in Numerical methods in fluid Dynamics, ed. Brezzi F., Lecture Notes in Mathematics*, vol. 1127, pp. 243–324, Spinger Verlag, Berlin, (1985)

[26] Schoenberg I.J., *Contributions to the problem of approximation of equidistant data by analytic function*, Part A, Quart. Appl. Math., vol. 4. pp. 45–99, (1946)

[27] Schumann U., Sweet R.A., *Direct Poisson Equation Solver for Potential and Pressure Fields on a Staggered Grid with Obstacles*, Lecture Notes in Physics, vol.59, pp. 397–403, (1976)

[28] Smith P.A., Stansby P.K., *Impulsively started flow around a circular cylinder by the vortex method*, J. Fluid Mech., vol. 194, pp.45–77, (1998)

[29] Thomann H., *Wind effects on buildings and structures*, American Scientist, vol.63, pp. 278–287, (1975)